

## Sensors

# Fluorescent Detection of 2,4-DNT and 2,4,6-TNT in Aqueous Media by Using Simple Water-Soluble Pyrene Derivatives

Igor S. Kovalev,<sup>[a]</sup> Olga S. Taniya,<sup>[a]</sup> Nataliya V. Slovesnova,<sup>[a, b]</sup> Grigory A. Kim,<sup>[c]</sup> Sougata Santra,<sup>[a]</sup> Grigory V. Zyryanov,<sup>\*,[a, c]</sup> Dmitry S. Kopchuk,<sup>[a, c]</sup> Adinath Majee,<sup>\*,[d]</sup> Valery N. Charushin,<sup>[a, c]</sup> and Oleg N. Chupakhin<sup>[a, c]</sup>

**Abstract:** Pyrene-containing water-soluble probes for the fluorescent detection of nitroaromatic compounds (NACs), such as explosive components (2,4-DNT and 2,4,6-TNT) and herbicides (2,4-dinitrocresol, 2,4-DNOC), in aqueous media are reported. In the probes, the introduction of surface-active hydrophilic “heads” at the periphery of lipophilic (i.e., hydrophobic) pyrene “tails” resulted in the formation of highly fluorescent micelle-like aggregates/pre-associates in aqueous solutions at concentrations of  $\leq 10^{-5}$  M. The en-

hanced fluorescence quenching of the herein reported architectures is achieved in the presence of ultra-trace amounts of TNT or 2,4-DNT with values of Stern–Volmer quenching constant close to  $1 \times 10^5 \text{ M}^{-1}$  and a detection limit as low as 182 ppb. The most hydrophilic probes demonstrated higher response to 2,4-DNT over TNT. Filter paper test strips impregnated with  $1 \times 10^{-5}$  M solutions of the probes were able to detect TNT, 2,4-DNT, and other NACs at levels as low as 50 ppb in water.

## Introduction

Sensing of nitroaromatic compounds (NACs), such as herbicides or pesticides (nitrocresols (NOCs)),<sup>[1]</sup> drugs, common components of explosives and explosive blends, such as TNT, 2,4-DNT, picric acid (PA) in drinking water, groundwater or seawater is very important for both human health protection<sup>[1]</sup> and for detecting buried unexploded ordnance or for locating underwater mines.<sup>[2,3]</sup> Environmental monitoring applications are based on the screening of soil and groundwater which are contaminated by toxic agricultural agents<sup>[1]</sup> or by nitro-explo-

sives in military bases.<sup>[4]</sup> According to the US Environmental Protection Agency (US EPA), the TNT level in drinking water needs to be lower than 2 ppb.<sup>[4]</sup> Hence, many techniques have been employed for the trace detection of nitro-explosives in solution such as GC/LC-MS,<sup>[6]</sup> ion mobility spectrometry, (IMS),<sup>[7]</sup> terahertz<sup>[8]</sup> or Raman<sup>[9]</sup> spectroscopy, electrochemical<sup>[10]</sup> or colorimetric detection,<sup>[11–14]</sup> detection by means of molecularly imprinted polymers (MIP),<sup>[15]</sup> and photoluminescence quenching methods.<sup>[2,3,13,14,16]</sup> Among the above mentioned methods, the direct fluorescence-quenching detection of NACs is now a well-established sensing technology.<sup>[13,14,16,17]</sup> The common mechanism of fluorescence quenching is based on photoinduced electron transfer (PET) from the excited fluorophore/chemosensor to the nitro-analyte.<sup>[14,16]</sup> The majority of nitro-explosives are strong fluorescence quenchers, which imparts their fast and selective fluorescence turn-off detection by using common fluorophores. Due to the high fluorescence quantum yield (up to 0.32)<sup>[18]</sup> and the ability to form stable donor–acceptor complexes with NACs,<sup>[19]</sup> pyrene derivatives are commonly used as fluorophores and/or single-molecule chemosensors for the visual detection of nitro- and some other explosives.<sup>[20,21]</sup> In addition, some pyrene-based hybrid materials, for example, films, fibers, silica microspheres, nanoparticles and crystalline wafers are widely studied as potential sensory elements for trace detection systems and devices for nitro-explosives.<sup>[14,16,22]</sup> For example, cellulose triacetate membranes with pyrene-1-butyric acid as fluorophore were used for screening of TNT, 2,4-DNT and hexogen (RDX) in groundwater.<sup>[23]</sup> Fang, Ding and co-authors have implemented pyrene fluorophores covalently attached to the glass surface to obtain

[a] Dr. I. S. Kovalev, O. S. Taniya, N. V. Slovesnova, Dr. S. Santra, Prof. G. V. Zyryanov, Dr. D. S. Kopchuk, Prof. V. N. Charushin, Prof. O. N. Chupakhin  
Chemical Engineering Institute  
Ural Federal University  
Yekaterinburg, K-2, 620002, 19 Mira Street (Russian Federation)  
E-mail: gvzyryanov@gmail.com

[b] N. V. Slovesnova  
Ural State Medical Academy  
of the Ministry of Health of the Russian Federation  
620014, Yekaterinburg, 3 Repina Street (Russian Federation)

[c] G. A. Kim, Prof. G. V. Zyryanov, Dr. D. S. Kopchuk, Prof. V. N. Charushin, Prof. O. N. Chupakhin  
I. Ya. Postovskiy Institute of Organic Synthesis  
Ural Division of the Russian Academy of Sciences  
22 S. Kovalevskoy Str., Yekaterinburg, 620219 (Russian Federation)

[d] Prof. A. Majee  
Department of Chemistry, Visva-Bharati (A Central University)  
Santiniketan-731235 (India)  
E-mail: adinath.majee@visva-bharati.ac.in

Supporting information for this article is available on the WWW under <http://dx.doi.org/10.1002/asia.201501310>.

a SAM film sensor for the detection of NACs in water, as well as in a gas phase.<sup>[24]</sup>

The heterophasic detection mode is the main disadvantage of the above approaches. Thus, prior to the binding event, the dissolved nitro-analyte must diffuse to the surface of the sensor (which is usually not soluble in water or polar solvents) and, after the binding has occurred, the signaling unit(s) (e.g., fluorophore(s)) will signal (via fluorescence quenching). So far, only few chemosensors soluble in polar solvents have been reported. For example, pyrene-1,3,6,8-tetralkylphosphoric acid and its ethyl ester were used for the fluorescent detection of TNT and PA in methanol, and high values of Stern–Volmer constants (up to  $8.3 \times 10^4 \text{ M}^{-1}$  for TNT) have been reported.<sup>[25]</sup>

Micellar solubilization is a powerful technique for improving both the sensitivity and solubility of non-water-soluble/hydrophobic chemosensors in aqueous environments. For instance, Anslyn and co-authors have developed a differentiated approach to the detection and identification of TNT, tetryl, RDX and octogen (HMX) in polar solvents by means of pyrene, and other PAH fluorophores sequestered in organic micelles.<sup>[26]</sup> Shi and co-authors reported an oligopyrene-based probe, oligo(2-(4-(1-pyrenyl)butanoyloxy)ethyltrimethylammonium bromide) (OPBEAB), for the fluorescent detection of TNT as low as  $7.0 \times 10^{-8} \text{ M}$  (70 ppb) in water in the presence of an anionic surfactant, sodium dodecyl sulphate (SDS). The high value of Stern–Volmer constant ( $K_{sv}^{\text{TNT}} = 5.3 \times 10^5 \text{ M}^{-1}$ ) was attributed to the formation of pseudo-micelles in aqueous solution.<sup>[27]</sup> Ding and co-authors utilized electrostatic interactions between bis-imidazolium tweezers-like pyrene probes and charged or neutral organic micelles to prove the determinative role of the type of micelles in adjusting fluorophore distribution in micellar solu-

tions, which influences the sensing behavior towards nitro-explosives in aqueous solutions.<sup>[28]</sup> Gho and co-authors reported unprecedentedly high binding constants due to the excimer fluorescence quenching by TNT ( $K_{sv}^{\text{TNT}} = 1 \times 10^6 \text{ M}^{-1}$ ) while using micellar solutions of tweezers-like pyrene derivative in semi-aqueous conditions.<sup>[29]</sup>

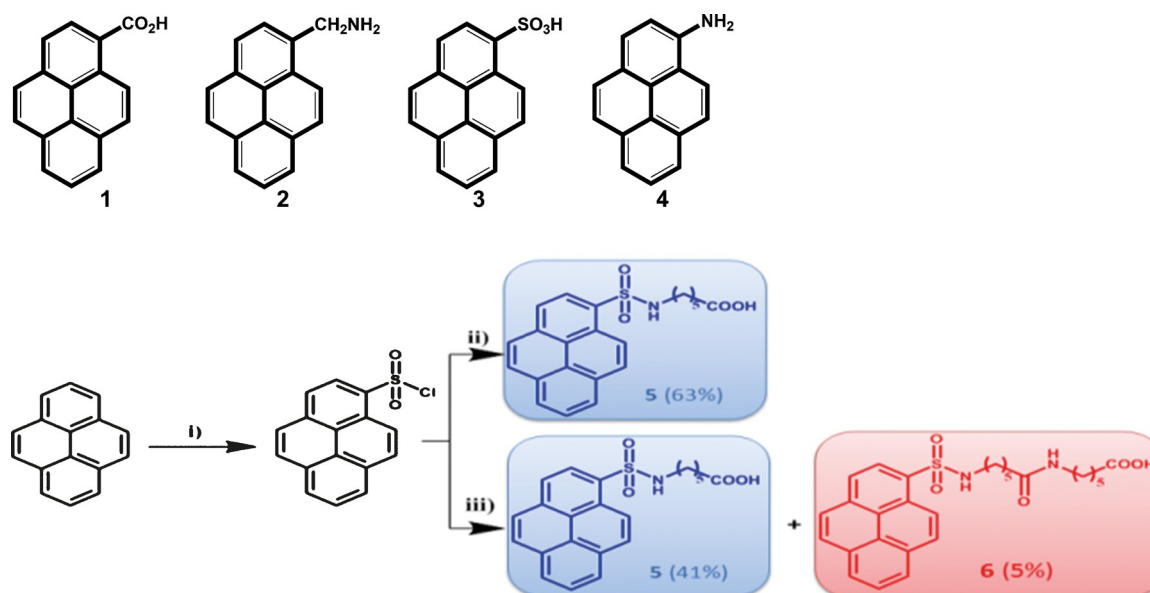
Herein, we report the synthesis and use of water-soluble pyrene derivatives 1–6 for the direct fluorescent detection of common explosives in aqueous solutions. The high selectivity and sensitivity have been confirmed by the enhanced fluorescence quenching of 1–6 in the presence of trace amounts of 2,4-DNT and 2,4,6-TNT.

## Results and Discussion

As a first step, we have synthesized some simple water-soluble pyrene derivatives (Scheme 1), such as pyrene-1-carboxylic acid 1 and 1-aminomethylpyrene 2 according to our previously reported approaches.<sup>[30]</sup> 1-Pyrenesulfonic acid 3 and 1-aminopyrene 4 have been prepared as described.<sup>[31]</sup>

In order to obtain water-soluble forms of compounds 1–4, the corresponding potassium (for 1,3) or TFA salts (for 2,4) were prepared *in situ*. Next, the photophysical properties of the probes 1–4 in aqueous solutions were investigated (Table 1, Figure 1).

The absorption spectra of chromophores 1–4 exhibited two major bands centered at ca. 270–280 nm and 350–360 nm, which are attributed to the electronic transitions between the  $S_0-S_2$  and  $S_0-S_1$  energy levels (Figure 1a). Except for compound 4, the emission spectra of all the chromophores are typical for the monomeric form of pyrene with the emission



i) 1.  $\text{H}_2\text{SO}_4$ ,  $\text{O}_2\text{NC}_6\text{H}_5$ . 2.  $\text{SOCl}_2$ , DMF; ii)  $\text{NaOOC}(\text{CH}_2)_5\text{NH}_2$  1.5 eqv, TBAB, THF (dry);  
iii)  $\text{NaOOC}(\text{CH}_2)_5\text{NH}_2$  3 eqv, TBAB, THF (dry).

**Scheme 1.** Structures of water-soluble pyrene derivatives 1–4 and synthetic route for the preparation of water-soluble pyrene derivatives 5–6.

**Table 1.** Photophysical properties and quenching constants for compounds 1–6.

Compd	$\lambda_{\text{abs}}$ [nm]	$\lambda_{\text{em}}$ [nm]	$\tau$ [ns]	$\Phi_F^{[a]}$	$K_{\text{sv}}^{\text{DNT}}$ [ $\text{M}^{-1}$ ]	$K_{\text{sv}}^{\text{TNT}}$ [ $\text{M}^{-1}$ ]
1 <sup>[b]</sup>	265, 276, 327, 342	384, 402	–	0.70	72 284	75 650
2 <sup>[c]</sup>	266, 277, 326, 343	379, 397	–	0.23	<b>68 951</b>	<b>83 041</b>
3 <sup>[b]</sup>	266, 277, 326, 343	379, 397	–	0.14	36 373	52 236
4 <sup>[c]</sup>	266, 277, 330, 345	446	–	0.07	21 189	46 022
5 <sup>[b]</sup>	285, 362	384, 402	11	0.76	34 189	33 325
6 <sup>[b]</sup>	269, 279, 351, 378	384, 402	12	0.78	83 480	33 784
					<b>94 802<sup>[d]</sup></b>	<b>66 134<sup>[d]</sup></b>

[a] Quinine sulfate in 0.1 N H<sub>2</sub>SO<sub>4</sub> used as a reference. [b] In form of potassium salt. [c] In form of TFA salt. [d] Measured at  $\lambda_{\text{ex}}$  = 345 nm. Best responses are marked in bold.

maxima centered at ca. 380 nm (Figure 1 b, Table 1, Figures S3, S9, and S15 in the Supporting Information). For compound 4, the shape and position of both the absorption and emission spectra are the same as described.<sup>[32]</sup> Depending on the nature of the 1-substituent, the fluorescence quantum yields for 1–4 vary from 0.07 to 0.70 (Table 1).

In aqueous solutions, compounds 1–4 exhibited a strong fluorescence response to TNT and 2,4-DNT. Figure 1 c depicts the most representative example of the spectrofluorimetric titration of TFA salt of compound 2 ( $1 \times 10^{-5}$  M) with increasing concentrations of TNT while exciting with UV light ( $\lambda_{\text{ex}}$  = 375 nm). Upon increasing the concentration of TNT, the fluorescence intensity of 2 gradually decreases, showing 60–70% quenching (Figure 1 b–c; Figures S10–S14, Supporting Information).

The data extracted from the SV plots indicate high values of Stern–Volmer constants for TNT ( $K_{\text{sv}}^{\text{TNT}} = 3.3\text{--}8.3 \times 10^4 \text{ M}^{-1}$ ) (Figure 1 c inset; Figures S6, S12, S18, and S24, Supporting Information). The linear response of the Stern–Volmer plot upon addition of TNT and 2,4-DNT suggests the high role of only one type of quenching, either static or dynamic, in the quenching process, and thus excludes the combination of both types of quenching at low concentrations of NACs.<sup>[16a]</sup>

A micellar solution of fluorophore is indeed more sensitive to the quenching by NACs than an equivalent concentration of fluorophore in a simple solvent.<sup>[26–29]</sup> Therefore, at the next step, aiming to improve the surface-active properties and impart hydrophilicity, we synthesized 6-(pyrene-1-ylsulfonamide)hexanoic acid 5 in 63% yield, starting from sodium salt of 6-aminocaproic acid by reacting with pyrene-1-sulfonyl chloride in absolute THF in the presence of Bu<sub>4</sub>NBr as a phase transfer catalyst (Scheme 1). 6-(6-(1-Pyrenesulfamido)hexanamide)hexanoic acid 6 was isolated only in 5% yield, along with product 5 (41%) and 1-pyrenesulfonic acid 3 (15%) by using the same reaction sequence in the presence of a higher amount (i.e. three-fold excess) of 6-aminocaproic acid salt. The occurrence of products 6 and 3 in the reaction mixture may be attributed to the equilibrium between the free acid 5 and its sodium salt under the phase transfer conditions in the presence of an excess of the sodium salt of 6-aminocaproic acid (see Scheme S1, Supporting Information). The calculated<sup>[33]</sup>  $\text{p}K_{\text{a}}$

values of acids 5–6 were also close:  $\text{p}K_{\text{a}}(5) = 3.72$  and  $\text{p}K_{\text{a}}(6) = 4.47$ .

The molecular structures of the obtained chemosensors 5–6 were confirmed by <sup>1</sup>H and <sup>13</sup>C NMR spectroscopies and by ESI-mass spectrometry (see the Supporting Information for details). In addition, single-crystal X-ray crystallography analysis of compound 5 has been performed to provide the most direct description of the molecular packing features.<sup>[34]</sup> According to Figure 2, 5 is packed in a head-to-head mode to form J-aggregates with a distance of ~3.5 Å between two pyrene rings, thus suggesting strong  $\pi$ – $\pi$ -interactions between them (Figure S59, Supporting Information).

The photophysical properties of compounds 5–6 were similar to those for 1–4. Indeed, it is expected that all six compounds in a water-based environment would exhibit more or less pronounced surface-active properties that are similar to surfactants, that is, due to the presence of the hydrophobic non-polar single tail of pyrene and the hydrophilic polar “head” of the corresponding acid (for 1, 3, 5–6) or quaternary amine group (for 2, 4) compounds 1–6 may accumulate at interfaces and produce aggregates (micelles or micelle-like architectures). On the other hand, according to both the X-ray data and the literature analysis, pyrene derivatives in a solid state or in a solution can aggregate through  $\pi$ – $\pi$  stacking to result in a reduction in the intensity of the emission.<sup>[35]</sup> We assumed that the introduction of longer chain surface-active moieties on the periphery of pyrene chromophores in aqueous media would restrict the formation of non-radiative pyrene aggregates due to the preferable formation of hydrophobic micelle-like aggregates/pre-associates. As a consequence, for the longer chain-modified compounds 5–6, we observed improvements of both photophysical properties and the sensor response towards NACs in aqueous solutions. Thus, the fluorescent quantum yield ( $\Phi_F$ ) of 5–6 increased up to 0.78 (Table 1). In addition, over 70% fluorescence quenching of 5–6 has been detected upon addition of 2,4-DNT or TNT (Figure 1 e; Figures S28–S38, Supporting Information). It is worthy to mention that, in contrast to compounds 1–4, fluorescent probes 5–6 demonstrated a higher sensory response to 2,4-DNT versus TNT. Thus, the Stern–Volmer constant value for 6 was calculated to be as high as  $K_{\text{sv}}^{\text{DNT}} = 9.5 \times 10^4 \text{ M}^{-1}$  (Table 1), and the fluorescence-quenching response can be detected at a concentration of 2,4-DNT ( $C_{\text{DNT}}$ ) as low as  $9.95 \times 10^{-7}$  M (182 ppb). In case of TNT, the highest calculated Stern–Volmer constant value was  $K_{\text{sv}}^{\text{TNT}} = 6.6 \times 10^4 \text{ M}^{-1}$  with a detection limit of 227 ppb. To the best of our knowledge, the Stern–Volmer constant values obtained for pyrene derivatives 1–6 in aqueous solution are close to or greater than those for pyrene derivatives employed for detection of NACs in aqueous solutions or polar solvents,<sup>[16, 26, 29, 36]</sup> except for the pseudo-micelle probe of OPBEAB/SDS reported by Shi et al., which resulted in a higher value ( $K_{\text{sv}}^{\text{TNT}} = 5.30 \times 10^5 \text{ M}^{-1}$ , limit of detection for TNT: 70 ppb). It is worthy to mention that, unlike the case reported herein, the efficiency of fluorescence quenching (i.e. the efficiency of PET between the OPBEAB/SDS probe and TNT) de-

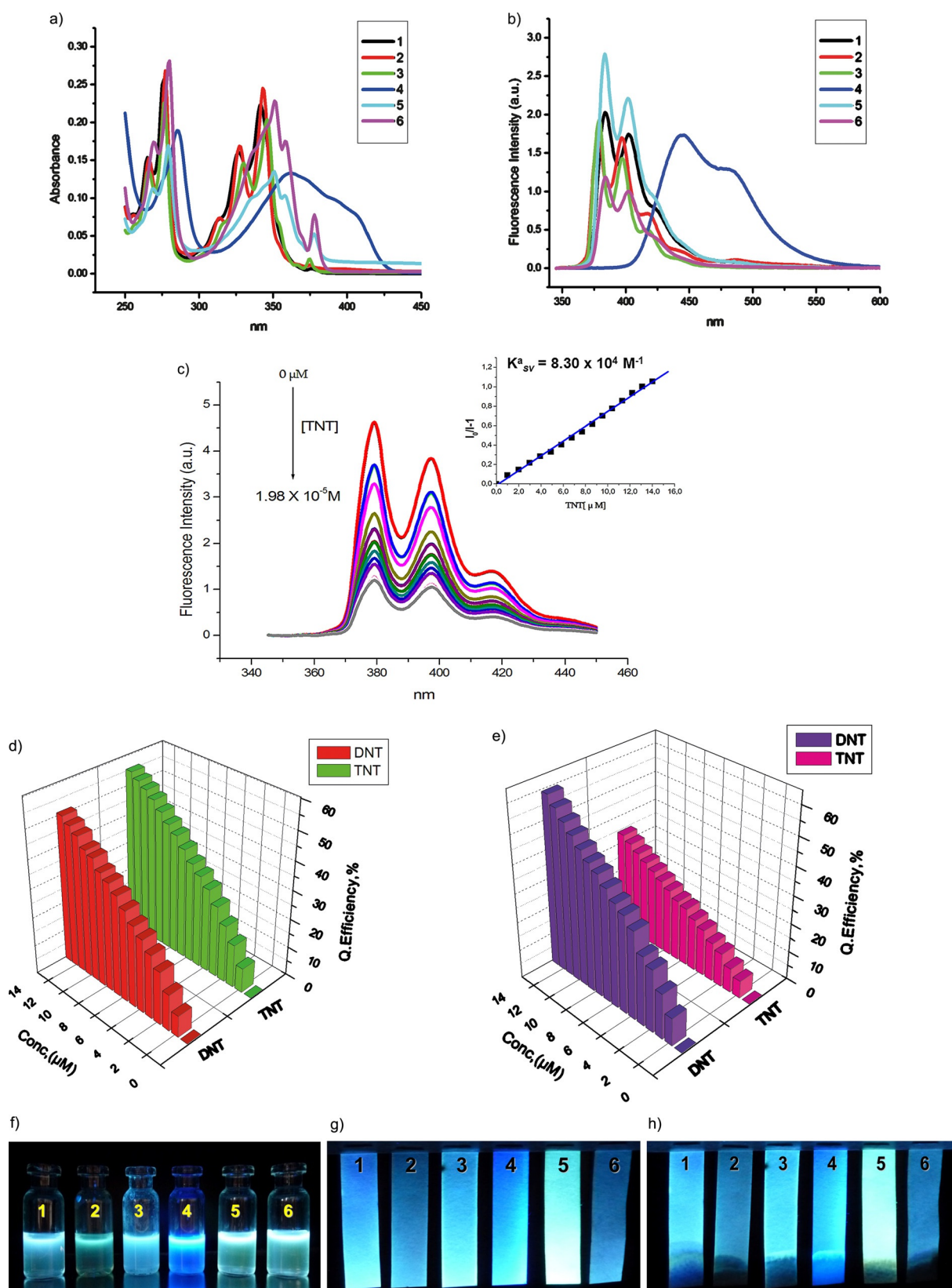


**Figure 1.** (a) UV absorption and (b) emission spectra of 1–6 in aqueous solutions ( $1 \times 10^{-5}$  M). (c) Emission spectra of 2 upon addition of TNT. The inset shows the Stern–Volmer plot. (d, e) Quenching efficiency of sensor 2 (d) and 6 (e) at different concentrations of 2,4-DNT and TNT. (f) Aqueous solutions of sensors 1–6 (from left to right,  $1 \times 10^{-5}$  M each) under UV light. (g) Paper strips, impregnated with aqueous solutions of sensors 1–6 (from left to right,  $1 \times 10^{-5}$  M) under UV light. (h) The same paper strips after short contact (10 sec.) with a solution of TNT in water (50 ppb) under UV light. (b–e) Wavelength of UV light:  $\lambda_{\text{ex}} = 375$  nm.



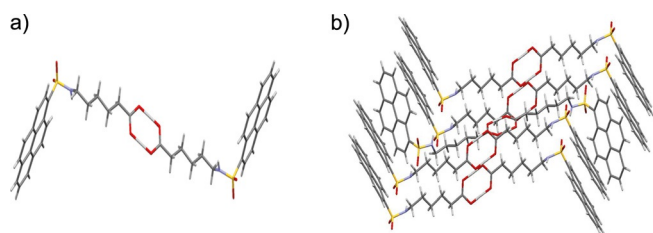


**Figure 2.** (a) Molecular structure of **5** (acetone). (b) Crystal packing in the structure of **5**.

depends strongly on the ratio of reagents and the mixing sequence due to the possibility of detachment of TNT molecules from the OPBEAB backbone, as suggested by the authors, and their trapping by the SDS micelle to decrease the quenching constants.<sup>[27]</sup> The same trend has been observed by Gho and co-authors for micellar solutions of tweezers-like pyrene derivative in semi-aqueous conditions.<sup>[29]</sup> In addition, none of the so far reported probes/sensors demonstrated a higher response to 2,4-DNT versus TNT in aqueous solutions.

The high quenching efficiency of the emission of chemosensors **5–6** upon the addition of TNT or 2,4-DNT can be attributed, as we may suggest, to the static quenching pattern due to the possible formation of a non-fluorescent donor–acceptor complex in a ground state *via* strong  $\pi$ – $\pi$  interactions between the nitroaromatic quencher and pyrene moieties of **5–6**. A possible role of collisional or dynamic quenching was ruled out based on the time-resolved fluorescence emission of compounds **5–6** (Figure S2, Table S1, Supporting Information). It was concluded that the decay lifetimes of chemosensors **5–6** were constant values of 11 ns (**5**) and 12 ns (**6**), being independent of the TNT concentration (Figure S2, Table S1, Supporting Information). This may confirm the quenching of the ground state of chemosensors **5–6** due to the PET process from excited fluorophores to NACs.<sup>[16,36]</sup> However, in the UV/Vis spectra of **5–6**, the absorbance bands from the pyrene moiety were found to be stable during the titration with NACs (Figures S41–S42, Supporting Information). These results may indicate a so-called false static quenching due to a “sphere of action”, where a molecule of NAC is near to the pyrene moiety (within the micelle or micelle-like architecture) at excitation, resulting in no fluorescence intensity from this moiety.<sup>[37]</sup> It is common that in “sphere of action” fluorescence quenching no ground state complex is formed.<sup>[37]</sup>

In order to explain the higher selectivity of probes **5–6** towards 2,4-DNT, we visualized the possible surface phenomena occurring in aqueous solutions of **1–6** (Figure 3, compound **5** is shown). Thus, at the concentrations of  $\leq 10^{-5}$  M, the self-association of compounds **1–6** affords micelle-like aggregates/pre-associates. Similarly to micelles, in these micelle-like architectures, the pyrene hydrophobic tails flock to the interior in order to minimize their contact with water, and the hydrophilic heads remain on the outer surface in order to maximize their contact with water.

In the center of these architectures the pyrene moieties are oriented with a distance between them higher than the typical distance accepted for  $\pi$ – $\pi$  interactions (i.e.,  $\sim 3.5$  Å). In our ex-

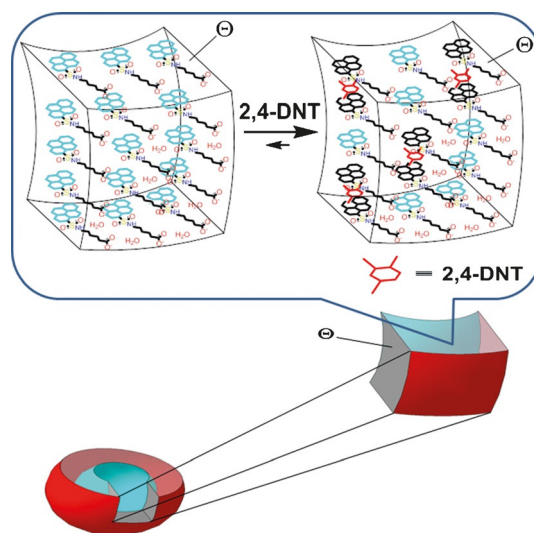


**Figure 3.** Bottom: The micelle-like aggregate of **5** in aqueous solution and the part of its elementary volume  $\Theta$ . Top: The possible quenching of the micelle-like aggregate due to the penetration of NACs (2,4-DNT) into the inner shell.

periments, we did not observe any emission at  $\sim 460$  nm which belongs to the emission of pyrene excimers.

Quenching of the emission of micelle-like aggregates/pre-associates of **1–6** in the presence of NACs was simulated for compound **5** and for 2,4-DNT as a quencher (Figure 3, top). 2,4-DNT is a fairly common component of many explosive mixtures and is an impurity in many explosive materials. The water solubility of 2,4-DNT is low (0.027 g/100 g at 22 °C), but still greater than that of TNT (0.013 g/100 g at 20 °C).<sup>[38]</sup> Both 2,4-DNT and TNT are hydrophobic molecules. Therefore, they are preferentially solubilized within the hydrophobic layer of the surfactant-like molecules of **1–6** rather than in the water phase. In this case, the electron-rich lipophilic (hydrophobic) environment of the central (pyrene) part of micelle-like aggregates/pre-associates of **1–6** acts as a driving force for the transport of polar molecules of NACs (e.g., 2,4-DNT). As a consequence, molecules of NACs will penetrate deep inside of these architectures in order to occupy the position in a close proximity to pyrene residues, causing the significant quenching of the fluorescence emission of pyrene fluorophores (Figure 1e, Figure 3).

The higher sensory response of probes **5–6** to 2,4-DNT over TNT can be attributed to the possible steric hindrances in case of TNT and to the lower dipole moment of TNT ( $D^{\text{DNT}} = 4.3$  D vs.  $D^{\text{TNT}} = 1.0$  D),<sup>[39]</sup> whereby molecules of 2,4-DNT would penetrate easier into the inner non-polar lipophilic shell of the micelle-like aggregates of **5–6** through the outer polar shell.

Tyndall scattering experiments (Figure 4), carried out for aqueous solutions of the most lipophilic probes **5–6**, with (Figure 4b,d) or without DNT (Figure 4a,c) added, further confirmed the formation of micelle-like architectures.

In addition to 2,4-DNT and TNT, sensors **1–6** showed good fluorescent response to other NACs, like 2,4-dinitroresol (DNOC) (Figure S39, Supporting Information), a common herbi-

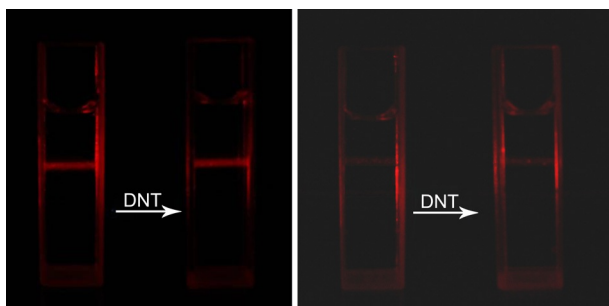


**Figure 4.** The Tyndall effect of the solutions ( $10^{-5}$  M) of **5** (a), **5** + 2,4-DNT (b), **6** (c), **6** + 2,4-DNT (d).

cide, while in the presence of non-planar and non-aromatic nitromethane (NM) or other nitroalkanes, only subtle changes in the fluorescence spectra were observed. For instance, for **6**, in the presence of a large excess of nitromethane, only about 5% quenching was observed (Figure S40, Supporting Information).

As a final step, in order to explore future practical applications of the herein reported probes **1–6**, paper-based test strips impregnated with aqueous solutions of **1–6** ( $1 \times 10^{-5}$  M) have been prepared (Figure 1 g, Figure S46, Supporting Information). After a short contact (within 10 seconds) with an aqueous solution of TNT (50 ppb), all the test strips displayed substantial fluorescence quenching (Figure 1 h), thus demonstrating the feasibility to visually detect NACs in water. Similar results were observed for 2,4-DNT, DNOC and other NACs.

## Conclusions

In summary, we have demonstrated fluorescent water-soluble pyrene derivatives for the efficient detection of common nitroaromatic explosives components, such as 2,4-DNT and TNT, in aqueous solutions. These probes demonstrated the dramatic fluorescent quenching over 70% in the presence of 2,4-DNT (182 ppb) or TNT (227 ppb) due to the possible formation of micelle-like aggregates/pre-associates at low concentrations ( $\leq 10^{-5}$  M). The most lipophilic probes **5–6** demonstrated a higher fluorescent response to 2,4-DNT versus TNT in aqueous solutions with values for Stern–Volmer constants up to  $9.5 \times 10^4 \text{ M}^{-1}$ . We believe that these new kinds of water-soluble probes, carrying both a non-polar pyrene tail and a polar quaternary amine or acid head, can greatly facilitate the design of simple and highly responsive materials for the detection of NACs in drinking water, groundwater, or seawater, as well as in other polar solvents. Further practical application of sensors **1–6** has been explored by preparing paper strips for the visual detection of NACs (as low as 50 ppb) in water.

## Experimental Section

### Materials and Reagents

All chemicals and reagents were used as received from commercial sources without further purification. Solvents for chemical synthesis were purified or freshly distilled prior to use, according to stan-

dard procedures. All chemical reactions were carried out under an inert atmosphere. The procedures for the synthesis of fluorophores **1–4** have been described previously.<sup>[30,31]</sup>

### Measurements and Characterizations

$^1\text{H}$  (400 MHz) and  $^{13}\text{C}$  NMR (100 MHz) spectra were measured on a Bruker Avance-400 spectrometer. Fluorescence spectra and fluorescence titration experiments were recorded on Horiba-Fluoromax-4 and Ocean Optics USB4000-FL spectrofluorometers. UV/Vis absorption spectra were recorded on a Shimadzu UV-2550 spectrophotometer.

### Acknowledgements

This work was supported by Russian Science Foundation (Ref. # 15-13-10033), by Act 211 Government of the Russian Federation (Ref. 02.A03.21.0006), and, for A.M., by the BRNS-DAE (Ref. # 37(2)/14/35/2014-BRNS/563, June 10, 2014).

**Keywords:** detection in aqueous media • explosives • fluorescence • fluorescence quenching • nitroaromatics

- [1] J. Stenersen in *Chemical Pesticides: Mode of Action and Toxicology*, CRC Press, Boca Raton, **2004**.
- [2] S. J. Toal, D. Magde, W. C. Trogler, *Chem. Commun.* **2005**, 5465.
- [3] T. Liu, K. Zhao, K. Liu, L. Ding, S. Yin, Y. Fang, *J. Hazard. Mater.* **2013**, 246–247, 52.
- [4] H. Sohn, R. M. Calhoun, M. J. Sailor, W. C. Trogler, *Angew. Chem. Int. Ed.* **2001**, 40, 2104; *Angew. Chem.* **2001**, 113, 2162.
- [5] US Department of Health and Human Services. Public Health Service; Agency for Toxic Substances and Disease Registry: 1995.
- [6] K. Håkansson, R. V. Coorey, R. A. Zubarev, V. L. Talrose, P. Hakansson, *J. Mass Spectrom.* **2000**, 35, 337.
- [7] T. Khayamian, M. Tabrizchi, M. Jafari, *Talanta* **2003**, 59, 327.
- [8] Z. Zhang, Y. Zhang, G. Zhao, C. Zhang, *Optik* **2007**, 118, 325.
- [9] J. M. Sylvia, J. A. Janni, J. D. Klein, K. M. Spencer, *Anal. Chem.* **2000**, 72, 5834.
- [10] M. Krausa, K. Schorb, *J. Electroanal. Chem.* **1999**, 461, 10.
- [11] R. T. Medary, *Anal. Chim. Acta* **1992**, 258, 341.
- [12] T. F. Jenkins, M. E. Walsh, *Talanta* **1992**, 39, 419.
- [13] S. J. Toal, W. C. Trogler, *J. Mater. Chem.* **2006**, 16, 2871.
- [14] Y. Salinas, R. Martóñez-Mañóñez, M. D. Marcos, F. Sanceno, A. M. Costero, M. Parra, S. Gil, *Chem. Soc. Rev.* **2012**, 41, 1261.
- [15] a) P. L. Edmiston, D. P. Campbell, D. S. Gottfried, J. Baughman, M. M. Timmers, *Sens. Actuators B* **2010**, 143, 574. For review see: b) Y. Ma, S. Xu, S. Wang, L. Wang, *TrAC Trends Anal. Chem.* **2015**, 67, 209.
- [16] For recent reviews see: a) G. V. Zyryanov, D. S. Kopchuk, I. S. Kovalev, E. V. Nosova, V. L. Rusinov, O. N. Chupakhin, *Russ. Chem. Rev.* **2014**, 83, 783; b) Z. Hu, B. J. Deibert, J. Li, *Chem. Soc. Rev.* **2014**, 43, 5815; c) Y. Ma, S. Wang, L. Wang, *TrAC Trends Anal. Chem.* **2015**, 65, 13; For reviews on fluorescence-based explosive detection by using pyrene derivatives, see: d) S. Shanmugaraju, P. S. Mukherjee, *Chem. Commun.* **2015**, 51, 16014; e) X. Sun, Y. Wang, Y. Lei, *Chem. Soc. Rev.* **2015**, 44, 8019.
- [17] a) J.-S. Yang, T. M. Swager, *J. Am. Chem. Soc.* **1998**, 120, 5321; b) J.-S. Yang, T. M. Swager, *J. Am. Chem. Soc.* **1998**, 120, 11864.
- [18] I. B. Berlman in *Handbook of Fluorescence Spectra of Aromatic Molecules*, Academic Press, New York, **1971**.
- [19] J. C. Barnes, J. A. Chudek, R. Fosma, F. Farrett, F. Mackie, J. Paton, D. R. Twisleton, *Tetrahedron* **1984**, 40, 1595.
- [20] J. V. Goodpaster, V. L. McGuffin, *Anal. Chem.* **2001**, 73, 2004.
- [21] S. Malashikhin, N. S. Finney, *J. Am. Chem. Soc.* **2008**, 130, 12846.
- [22] R. V. Taudte, A. Beavis, L. Wilson-Wilde, C. Roux, P. Doble, L. Blanes, *Lab Chip* **2013**, 13, 4164.
- [23] C. Jian, W. R. Seitz, *Anal. Chim. Acta* **1990**, 237, 265.

- [24] a) S. Zhang, F. Lü, L. Gao, L. Ding, Y. Fang, *Langmuir* **2007**, *23*, 1584; b) L. Ding, Y. Liu, Y. Cao, L. Wang, Y. Xin, Y. Fang, *J. Mater. Chem.* **2012**, *22*, 11574.
- [25] N. Venkatramaiah, A. D. G. Firmino, F. A. A. Paz, J. P. C. Tomé, *Chem. Commun.* **2014**, *50*, 9683.
- [26] A. D. Hughes, I. C. Glenn, A. D. Patrick, A. Ellington, E. V. Anslyn, *Chem. Eur. J.* **2008**, *14*, 1822.
- [27] Y. Chen, H. Bai, Q. Chen, C. Li, G. Shi, *Sens. Actuators B* **2009**, *138*, 563.
- [28] L. Ding, Y. Bai, Y. Cao, G. Ren, G. J. Blanchard, Y. Fang, *Langmuir* **2014**, *30*, 7645.
- [29] J.-H. Hong, J.-H. Choi, D.-G. Cho, *Bull. Korean Chem. Soc.* **2014**, *35*, 3158.
- [30] I. S. Kovalev, N. V. Slovesnova, D. S. Kopchuk, G. V. Zyryanov, O. S. Taniya, V. L. Rusinov, O. N. Chupakhin, *Russ. Chem. Bull.* **2014**, *63*, 1312.
- [31] a) F. M. Menger, L. G. Whitesell, *J. Org. Chem.* **1987**, *52*, 17; b) M. Orłowska, M. Mroczkiewicz, K. Guzow, R. Ostaszewski, A. M. Klonkowski, *Tetrahedron* **2010**, *66*, 2486.
- [32] H. Chakraborti, K. Bramhaiah, N. S. John, S. K. Pal, *Phys. Chem. Chem. Phys.* **2013**, *15*, 19932.
- [33] Marvin was used for calculations of  $pK_a$ , Marvin 5.11.1, **2013**, ChemAxon (<http://www.chemaxon.com>).
- [34] CCDC 1415335 contains the supplementary crystallographic data for this paper. These data can be obtained free of charge from The Cambridge Crystallographic Data Centre.
- [35] J. A. Mikroyannidis, L. Fenenko, C. Adachi, *J. Phys. Chem. B* **2006**, *110*, 20317.
- [36] a) Y. Wang, A. La, C. Brückner, Y. Lei, *Chem. Commun.* **2012**, *48*, 9903; b) W. Chen, N. B. Zuckerman, J. P. Konopelski, S. Chen, *Anal. Chem.* **2010**, *82*, 461.
- [37] a) J. R. Lakowicz in *Principles of Fluorescence Spectroscopy*, 3rd ed., Springer, New York, USA, **2006**; b) J. Keizer, *J. Am. Chem. Soc.* **1983**, *105*, 1494.
- [38] V. L. Zbarskii, V. F. Zhilin in *Toluol i ego nitroproizvodnye (Toluene and its nitro-derivatives)*, Editorial URSS, Moscow, **2000**.
- [39] R. C. Gass, H. Spedding, H. D. Springal, *J. Chem. Soc.* **1957**, 3455.

Manuscript received: November 24, 2015

Revised: January 10, 2016

Accepted Article published: January 12, 2016

Final Article published: February 2, 2016